Organometallics 1991, 10, 2239–2247

Chemistry of Iridium Carbonyl Cluster Complexes. Synthesis and Characterization of Mixed-Metal Carbonyl Clusters via Capping Reactions with $HgCl_2$ and $Au(PPh_3)Cl$. Crystal Structures of $[N(PPh_3)_2][Ir_6(\mu_3\text{-}CO)_3(CO)_{12}(\mu_3\text{-}HgCl)]\cdot 0.5C_6H_{12}$ and $[NMe_3(CH_2Ph)][Ir_6(\mu\text{-}CO)_3(CO)_{12}[\mu_3\text{-}Au(PPh_3)]]\cdot C_4H_8O$

Roberto Della Pergola,[1a] Francesco Demartin,[1b] Luigi Garlaschelli,*[1a] Mario Manassero,[1b]
Secondo Martinengo,[1a] Norberto Masciocchi,*[1b] and Mirella Sansoni[1b]

Dipartimento di Chimica Inorganica e Metallorganica and Istituto di Chimica Strutturistica Inorganica, Università di Milano, via G. Venezian 21, I-20133 Milano, Italy

Received March 16, 1990

The new anionic carbonyl clusters $[Ir_6(CO)_{15}(HgCl)]^-$ (1) and $[Ir_6(CO)_{15}[Au(PPh_3)]]^-$ (2) have been obtained by reaction of $[Ir_6(CO)_{15}]^{2-}$ with $HgCl_2$ or $Au(PPh_3)Cl$ in tetrahydrofuran solution. The complexes have been characterized by IR(ν_{CO}) and NMR studies (^{13}C, ^{31}P, ^{199}Hg) and fast atom bombardment mass spectroscopy. The molecular structures of complexes 1 and 2 have been determined by single-crystal X-ray diffraction. The salt $[N(PPh_3)_2][Ir_6(\mu_3\text{-}CO)_3(CO)_{12}(\mu_3\text{-}HgCl)]\cdot 0.5C_6H_{12}$ (**1a**) crystallizes in the triclinic space group $P\bar{1}$, with unit cell dimensions a = 14.115 (5) Å, b = 14.619 (3) Å, c = 17.762 (5) Å, α = 71.21 (2)°, β = 66.43 (2)°, γ = 64.61 (2)°, and Z = 2; R = 0.039 and R_w = 0.044 for 4513 observed reflections. The salt $[NMe_3(CH_2Ph)][Ir_6(\mu\text{-}CO)_3(CO)_{12}[\mu_3\text{-}Au(PPh_3)]]\cdot C_4H_8O$ (**2a**) crystallizes in the triclinic space group $P\bar{1}$, with unit cell dimensions a = 13.582 (2) Å, b = 14.513 (2) Å, c = 14.624 (4) Å, α = 110.07 (2)°, β = 91.75 (2)°, γ = 98.37 (1)°, and Z = 2; R = 0.033 and R_w = 0.043 for 6011 observed reflections. The heptanuclear cluster 1 has an octahedral iridium core, with the mercury atom, which bears a terminally bonded chlorine ligand, capping a triangular face [Ir–Hg average value 2.792 Å, Hg–Cl 2.346 (5) Å]. Two terminal CO groups are bound to each iridium atom, while the three face-bridging carbonyl groups connect vertex-sharing faces. Average distances are Ir–Ir 2.797 Å, Ir–CO_t 1.86 Å, Ir–CO_b 2.23 Å (t = terminal, b = bridging). The structural analysis of 2 shows that the $AuPPh_3$ group caps one face of the Ir_6 octahedral framework [Ir–Au average 2.838 Å, Au–P 2.272 (3) Å], maintaining the stereogeometry of the CO ligands of the parent metal carbonyl anion $[Ir_6(CO)_{15}]^{2-}$ of idealized D_3 symmetry. Average distances are Ir–Ir 2.796 Å, Ir–CO_t 1.87 Å, Ir–CO_b 2.08 Å. The μ-CO groups in 2 are bent, so to assume a "semitriple" coordination mode. Very little difference in the ligands' environments is present in the two clusters.

Introduction

In the course of our studies on the chemistry of the red isomer[2a,3] of $Ir_6(CO)_{16}$ under various chemical conditions, we found that the hexanuclear carbonyl reacts with neutral and anionic ligands with substitution of one or more carbon monoxide groups.[4-9] X-ray analysis showed that the basic structure of $Ir_6(CO)_{16}$ is significantly modified and that the substituted products contain different dispositions and coordination modes for the remaining carbonyl ligands so that edge-bridging carbonyls appear.

We also investigated the reactions of the hexanuclear dianion $[Ir_6(CO)_{15}]^{2-}$[2b,10] with halogens, $FeCl_3$, and group 11 metal cations such as Ag^+ and $[Cu(NCMe)_4]^+$. The reaction with halogens and $FeCl_3$ afforded hexanuclear substituted anionic iridium carbonyl clusters such as $[Ir_6(CO)_{14}X]^-$ (X = Cl, Br, I) and $[Ir_6(CO)_{15}Cl]^-$, identical with those obtained or observed as intermediate species in the substitution reactions on the neutral carbonyl.[8,9] The reaction of $[Ir_6(CO)_{15}]^{2-}$ with Ag^+ or $[Cu(NCMe)_4]^+$ does not incorporate the coinage metals into the metal framework; instead, it gives the first high nuclearity iridium carbonyl cluster, namely $[Ir_{12}(CO)_{26}]^{2-}$.[11] In this paper we report the details of the reaction of $[Ir_6(CO)_{15}]^{2-}$ with $HgCl_2$ and $Au(PPh_3)Cl$ in the synthesis of the anions 1 and 2, $[Ir_6(CO)_{15}(HgCl)]^-$ and $[Ir_6(CO)_{15}[Au(PPh_3)]]^-$, both containing a heptanuclear heterometallic core. A complete X-ray structural analysis of the two derivatives $[N(PPh_3)_2][Ir_6(\mu_3\text{-}CO)_3(CO)_{12}(\mu_3\text{-}HgCl)]\cdot 0.5C_6H_{12}$ (**1a**) and $[NMe_3(CH_2Ph)][Ir_6(\mu\text{-}CO)_3(CO)_{12}[\mu_3\text{-}Au(PPh_3)]]\cdot C_4H_8O$ (**2a**) is also reported. The fluxional behavior of 1 and 2 has been studied by ^{13}C NMR spectroscopy.

Results and Discussion

Synthesis of $[Ir_6(CO)_{15}(HgCl)]^-$ and $[Ir_6(CO)_{15}[Au(PPh_3)]]^-$. Treatment of a tetrahydrofuran (THF) solution of the hexanuclear cluster $[Ir_6(CO)_{15}]^{2-}$ with a stoichiometric amount of $HgCl_2$ under nitrogen atmosphere at room temperature, results in the formation of a red-brown solution which contains the anion 1, which has been isolated by adding cyclohexane to the THF solution and

---

(1) (a) Dipartimento di Chimica Inorganica e Metallorganica. (b) Istituto di Chimica Strutturistica Inorganica.

(2) (a) Malatesta, L.; Caglio, G.; Angoletta, M. *Chem. Commun.* **1970**, 532. (b) Angoletta, M.; Malatesta, L.; Caglio, G. *J. Organomet. Chem.* **1975**, *94*, 99.

(3) Garlaschelli, L.; Martinengo, S.; Bellon, P. L.; Demartin, F.; Manassero, M.; Chiang, M. Y.; Wei, C. Y.; Bau, R. *J. Am. Chem. Soc.* **1984**, *106*, 6664.

(4) Demartin, F.; Manassero, M.; Sansoni, M.; Garlaschelli, L.; Sartorelli, U.; Tagliabue, F. *J. Organomet. Chem.* **1982**, *234*, C39.

(5) Demartin, F.; Manassero, M.; Sansoni, M.; Garlaschelli, L.; Raimondi, C. C.; Martinengo, S. *J. Organomet. Chem.* **1983**, *243*, C10.

(6) Demartin, F.; Manassero, M.; Sansoni, M.; Garlaschelli, L.; Malatesta, M. C.; Sartorelli, U. *J. Organomet. Chem.*, **1983**, *248*, C17.

(7) Garlaschelli, L.; Malatesta, M. C.; Martinengo, S.; Demartin, F.; Manassero, M.; Sansoni, M. *J. Chem. Soc., Dalton Trans.* **1986**, 777.

(8) Della Pergola, R.; Garlaschelli, L.; Martinengo, S.; Demartin, F.; Manassero, M.; Masciocchi, N. *J. Chem. Soc., Dalton Trans.* **1988**, 2307.

(9) Della Pergola, R.; Demartin, F.; Garlaschelli, L.; Manassero, M.; Martinengo, S.; Masciocchi, N. *J. Organomet. Chem.* **1990**, *396*, 385.

(10) Demartin, F.; Manassero, M.; Sansoni, M.; Garlaschelli, L.; Martinengo, S.; Canziani, F. *J. Chem. Soc., Chem. Commun.* **1980**, 903.

(11) Della Pergola, R.; Demartin, F.; Garlaschelli, L.; Manassero, M.; Martinengo, S.; Sansoni, M. *Inorg. Chem.* **1987**, *26*, 3487.

0276-7333/91/2310-2239$02.50/0

Table I. Selected Distances (Å) in the Monoanion $[Ir_6(CO)_{15}(HgCl)]^-$ with Estimated Standard Deviations (Esd's) on the Last Figure in Parentheses[a,b]

	Metal–Metal		
Hg–Ir(1)	2.796 (1)	Ir(2)–Ir(5)	2.768 (1)
Hg–Ir(2)	2.788 (1)	Ir(2)–Ir(6)	2.750 (1)
Hg–Ir(3)	2.796 (1)	Ir(3)–Ir(4)	2.764 (1)
Ir(1)–Ir(2)	2.889 (1)	Ir(3)–Ir(6)	2.767 (1)
Ir(1)–Ir(3)	2.891 (1)	Ir(4)–Ir(5)	2.777 (1)
Ir(1)–Ir(4)	2.768 (1)	Ir(4)–Ir(6)	2.777 (1)
Ir(1)–Ir(5)	2.754 (1)	Ir(5)–Ir(6)	2.775 (1)
Ir(2)–Ir(3)	2.879 (1)		
	Ir–C_t		
Ir(1)–C(11)	1.85 (2)	Ir(4)–C(41)	1.79 (3)
Ir(1)–C(12)	1.89 (2)	Ir(4)–C(42)	1.84 (2)
Ir(2)–C(21)	1.85 (2)	Ir(5)–C(51)	1.86 (2)
Ir(2)–C(22)	1.84 (2)	Ir(5)–C(52)	1.88 (2)
Ir(3)–C(31)	1.88 (2)	Ir(6)–C(61)	1.88 (2)
Ir(3)–C(32)	1.83 (2)	Ir(6)–C(62)	1.88 (2)
	Ir–C_b		
Ir(1)–CT(1)	2.10 (2)	Ir(6)–CT(2)	2.25 (2)
Ir(4)–CT(1)	2.36 (2)	Ir(3)–CT(3)	2.08 (2)
Ir(5)–CT(1)	2.25 (2)	Ir(4)–CT(3)	2.32 (2)
Ir(2)–CT(2)	2.06 (2)	Ir(6)–CT(3)	2.26 (2)
Ir(5)–CT(2)	2.36 (2)		
	Other Distances		
C–O_t*	1.15	Hg–Cl	2.346 (5)
C–O_b*	1.18		

[a] Starred bonds are equated with averages values. [b] Abbreviations for atoms in Tables I–IV: t = terminal; b = bridging; CT = triple (face) bridging carbon; OT = triple (face) bridging carbon; CD = double (edge) bridging carbon; OD = double (edge) bridging oxygen.

partially removing the solvents under vacuum. The infrared spectrum of this complex, in THF solution, exhibits bands at 2088 (w), 2044 (s), 2004 (w), and 1765 (m) cm^{-1} (Figure 1a), in agreement with the presence of terminal as well as face-bridging carbonyl groups. As expected, the terminal CO absorption bands are shifted 50–60 cm^{-1} to higher wavenumbers with respect to those of $[Ir_6(CO)_{15}]^{2-}$.

Anion 1 gives no detectable reaction when submitted to 1 atm of carbon monoxide for 24 h at 25 °C. It reacts with a stoichiometric amount of iodine, giving the substituted derivative $[Ir_6(CO)_{15}I]^-$ according to

$$[Ir_6(CO)_{15}(HgCl)]^- + I_2 \rightarrow [Ir_6(CO)_{15}I]^- + HgClI$$

The formation of the halide-substituted cluster has been established by comparison of the IR spectra.[8,9]

When the anionic cluster $[Ir_6(CO)_{15}]^{2-}$ is reacted with other mercury sources, such as EtHgCl, $Hg(MeCO_2)_2$, or Hg_2Cl_2, the reaction course is different and produces different compounds, presently under investigation.

Anion 2 is quantitatively obtained, at room temperature, by reacting a solution of the cation $[Au(PPh_3)]^+$ (prepared by reaction of $Au(PPh_3)Cl$ with $Ag[BF_4]$ in THF) with $[NMe_3(CH_2Ph)]_2[Ir_6(CO)_{15}]$ in a 1:1 molar ratio. The product is recovered as a reddish precipitate by addition of cyclohexane to the THF solution.

The dianion $[Ir_6(CO)_{15}]^{2-}$ does not react quantitatively with $Au(PPh_3)Cl$ in THF even in the presence of a large excess of $Au(PPh_3)Cl$ (molar ratio 1:6) and at reflux. This is due to the existence of the equilibrium

$$[Ir_6(CO)_{15}]^{2-} + Au(PPh_3)Cl \rightleftarrows [Ir_6(CO)_{15}[Au(PPh_3)]]^- + Cl^-$$

This equilibrium is in agreement with the observation that when anion 2 is dissolved in CH_2Cl_2 in the presence of $[N(PPh_3)_2]Cl$, the chloride ion displaces the $[Au(PPh_3)]^+$ fragment, generating $[Ir_6(CO)_{15}]^{2-}$ and $Au(PPh_3)Cl$. This type of equilibrium has been already observed in rhodium carbonyl carbide clusters.[12]

Table II. Selected Angles (deg) in the Monoanion $[Ir_6(CO)_{15}(HgCl)]^-$ with Esd's on the Last Figure in Parentheses[a]

	Ir–Hg–Ir		
Ir(1)–Hg–Ir(2)	62.31 (3)	Ir(2)–Hg–Ir(3)	62.07 (3)
Ir(1)–Hg–Ir(3)	62.26 (3)		
	Ir–C_b–Ir		
Ir(1)–CT(1)–Ir(4)	73.6 (6)	Ir(5)–CT(2)–Ir(6)	74.0 (5)
Ir(1)–CT(1)–Ir(5)	78.4 (6)	Ir(3)–CT(3)–Ir(4)	77.6 (6)
nIr(4)–CT(1)–Ir(5)	74.1 (5)	Ir(3)–CT(3)–Ir(6)	78.9 (6)
Ir(2)–CT(2)–Ir(5)	77.1 (6)	Ir(4)–CT(3)–Ir(6)	74.6 (6)
Ir(2)–CT(2)–Ir(6)	79.1 (6)		
	Ir–C_b–O		
Ir(1)–CT(1)–OT(1)	136 (1)	Ir(6)–CT(2)–OT(2)	134 (1)
Ir(4)–CT(1)–OT(1)	131 (1)	Ir(3)–CT(3)–OT(3)	136 (2)
Ir(5)–CT(1)–OT(1)	135 (2)	Ir(4)–CT(3)–OT(3)	134 (1)
Ir(2)–CT(2)–OT(2)	138 (1)	Ir(6)–CT(3)–OT(3)	132 (1)
Ir(5)–CT(2)–OT(2)	130 (1)		
	Ir–C_t–O*		

[a] Starred angle is equated with an average value.

Table III. Selected Distances (Å) in the Monoanion $[Ir_6(CO)_{15}[Au(PPh_3)]]^-$ with Esd's on the Last Figure in Parentheses[a]

	Metal–Metal		
Au–Ir(1)	2.820 (1)	Ir(2)–Ir(5)	2.801 (1)
Au–Ir(2)	2.844 (1)	Ir(2)–Ir(6)	2.738 (1)
Au–Ir(3)	2.850 (1)	Ir(3)–Ir(4)	2.732 (1)
Ir(1)–Ir(2)	2.877 (1)	Ir(3)–Ir(6)	2.815 (1)
Ir(1)–Ir(3)	2.851 (1)	Ir(4)–Ir(5)	2.788 (1)
Ir(1)–Ir(4)	2.802 (1)	Ir(4)–Ir(6)	2.792 (1)
Ir(1)–Ir(5)	2.719 (1)	Ir(5)–Ir(6)	2.785 (1)
Ir(2)–Ir(3)	2.847 (1)		
	Ir–C_t		
Ir(1)–C(11)	1.90 (1)	Ir(4)–C(41)	1.89 (1)
Ir(1)–C(12)	1.86 (1)	Ir(4)–C(42)	1.84 (1)
Ir(2)–C(21)	1.89 (1)	Ir(5)–C(51)	1.85 (1)
Ir(2)–C(22)	1.87 (1)	Ir(5)–C(52)	1.86 (1)
Ir(3)–C(31)	1.88 (1)	Ir(6)–C(61)	1.86 (1)
Ir(3)–C(32)	1.88 (1)	Ir(6)–C(62)	1.88 (1)
	Ir–C_b		
Ir(1)–CD(1)	2.06 (1)	Ir(6)–CD(2)	2.11 (1)
Ir(5)–CD(1)	2.13 (1)	Ir(3)–CD(3)	2.06 (1)
Ir(2)–CD(2)	2.10 (1)	Ir(4)–CD(3)	2.11 (1)
	Other Distances		
Au–P	2.272 (3)	C–O_b*	1.16
C–O_t*	1.14		

[a] Starred bonds are equated with average values.

The infrared CO absorption bands of 2 are shifted to higher wavenumbers with respect to those of $[Ir_6(CO)_{15}]^{2-}$ in agreement with the lower electron density on the monoanionic cluster; the complex exhibits bands at 2062 (vw), 2018 (vs), 1978 (vw), 1952 (vw), and 1790 (m) cm^{-1} (THF solution, Figure 1b).

Salts of 1 and 2 are moderately air-stable in the solid state as well as in solution; they are very soluble in THF, acetone, and CH_2Cl_2, sparingly soluble in alcohols, and insoluble in aliphatic or aromatic hydrocarbons.

Crystal Structures of $[N(PPh_3)_2][Ir_6(\mu_3\text{-}CO)_3(CO)_{12}(\mu_3\text{-}HgCl)]\cdot 0.5C_6H_{12}$ (1a) and $[NMe_3(CH_2Ph)][Ir_6(\mu\text{-}CO)_3(CO)_{12}[\mu_3\text{-}Au(PPh_3)]]\cdot C_4H_8O$ (2a). The solid-state structures of compounds 1a and 2a, determined by X-ray single-crystal diffraction, consist of a packing of discrete cations and anions in a 1:1 molar ratio with normal van der Waals contacts. The crystals of 1a contain one C_6H_{12}, and those of 2a, two C_4H_8O clathrated molecules per unit cell.

---

(12) Fumagalli, A.; Martinengo, S.; Albano, V. G.; Braga, D.; Grepioni, F. *J. Chem. Soc., Dalton Trans.* **1989**, 2343.

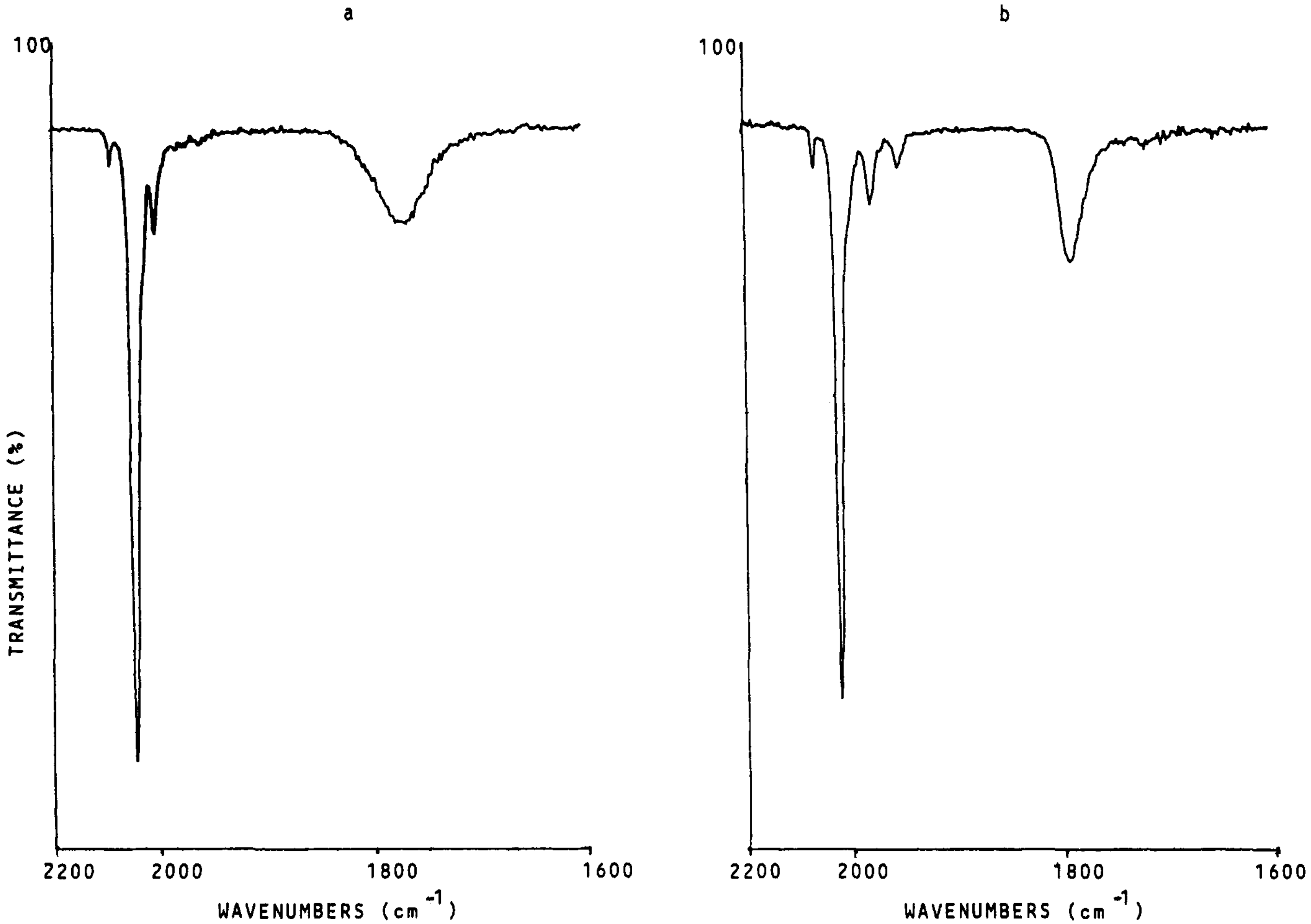

Figure 1. (a) Infrared spectrum of $[N(PPh_3)_2][Ir_6(CO)_{15}(HgCl)]$ in THF solution. (b) Infrared spectrum of $[N(PPh_3)_2][Ir_6(CO)_{15}[Au(PPh_3)]]$ in THF solution.

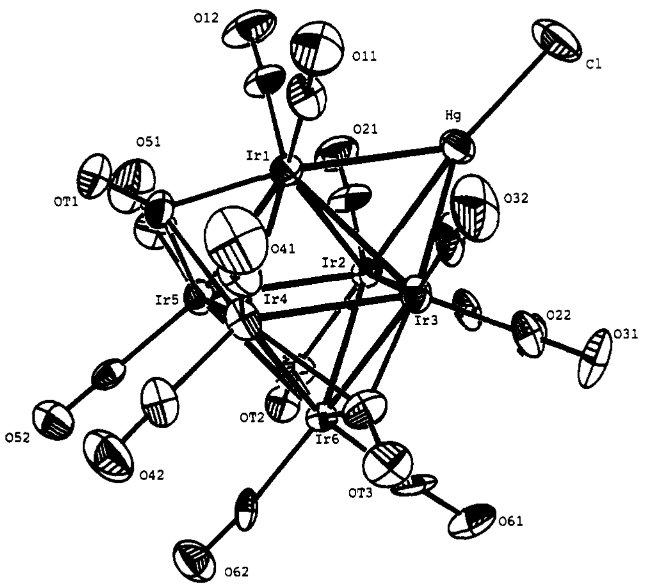

Figure 2. ORTEP drawing and atom-labeling scheme for $[Ir_6(CO)_{15}(HgCl)]^-$. Thermal ellipsoids are drawn at 30% probability. Carbonyl carbons are designated in a manner analogous to the oxygens to which they are attached.

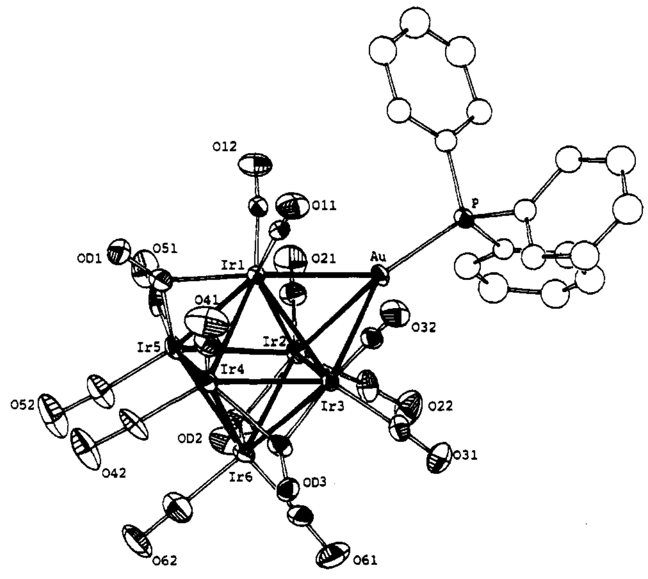

Figure 3. ORTEP drawing and atom-labeling scheme for $[Ir_6(CO)_{15}[Au(PPh_3)]]^-$. Thermal ellipsoids are drawn at 30% probability. Carbonyl carbons are designated in a manner analogous to the oxygens to which they are attached.

The molecular structures for the anions 1 and 2 are shown in Figures 2 and 3, respectively, together with the atom-labeling scheme. Selected bond distances and angles are listed in Tables I–IV, respectively. The metal skeleton of the two clusters consists of an octahedron of iridium atoms with one face [Ir(1)–Ir(2)–Ir(3)] capped by a Hg–Cl moiety for 1 and by a $Au(PPh_3)$ fragment for 2. Mercury can bond to a carbonyl cluster in a variety of fashions. The most familiar metal–mercury bond linkages are linear[13] or with connectivity from two to six,[14] but only very few

---

[13] For same examples see: (a) Mays, M. J.; Robb, J. D. J. *J. Chem. Soc.* A **1968**, 329. (b) Deutcher, J.; Fadel, S.; Ziegler, M. L. *Angew. Chem., Int. Ed. Engl.* **1977**, *16*, 704. (c) Glockling, F.; Mahole, V. B.; Sweeney, J. J. J. *J. Chem. Soc., Dalton Trans.* **1979**, 767.

Table IV. Selected Angles (deg) in the Anion $[Ir_6(CO)_{15}[Au(PPh_3)]]^-$ with Esd's on the Last Figure in Parentheses[a]

	Ir–Au–Ir		
Ir(1)–Au–Ir(2)	61.05 (2)	Ir(2)–Au–Ir(3)	60.01 (1)
Ir(1)–Au–Ir(3)	60.37 (1)		
	Ir–C_b–Ir		
Ir(1)–CD(1)–Ir(5)	80.9 (5)	Ir(3)–CD(3)–Ir(4)	81.9 (4)
Ir(2)–CD(2)–Ir(6)	81.2 (4)		
	Ir–C_b–O		
Ir(1)–CD(1)–OD(1)	140 (1)	Ir(6)–CD(2)–OD(2)	138 (1)
Ir(5)–CD(1)–OD(1)	135 (1)	Ir(3)–CD(3)–OD(3)	140 (1)
Ir(2)–CD(2)–OD(2)	138 (1)	Ir(4)–CD(3)–OD(3)	136 (1)
Ir–C_t–O*	177		

[a] Starred angle is equated with an average value.

examples have been reported where the mercury atom links only a triangular face of a carbonyl cluster.[15] On the other hand, $Au(PPh_3)$ usually caps triangular faces of the clusters,[16] although edge bridges are also common.[17]

The average Ir–Ir interactions are statistically identical in the two cases (2.797 Å in **1**, 2.796 Å in **2**), but the Ir–Ir bond distances within each metal core are affected by the presence of the heteroatom; specifically, the metal-capped Ir–Ir distances (average 2.886 Å for **1**, 2.858 Å for **2**) are longer than the uncapped ones (average 2.767 Å for **1**, 2.774 Å for **2**). In the case of Ir clusters the effect of the μ-CO groups on the corresponding Ir–Ir bond lengths is controversial: sometimes it is definitely elongating;[3,18] sometimes it causes elongation and shortening of the Ir–Ir vectors of the same complex.[2–10] In the anion **2**, on the contrary, the edge-bridging groups have a relevant shortening effect with an average Ir–Ir of 2.73 Å. The average Ir–Au separation (2.837 Å) is longer than the average Ir–Hg (2.793 Å), and these values are longer than the corresponding separations found in other Ir–Au[19] and Ir–Hg[20] complexes where the heteroatoms are not face-capping. The terminal carbonyl group stereogeometry of the parent dianion[10] is maintained, and in both compounds, each iridium atom is bonded to two terminal CO groups, which show little deviation from linearity (M–C–O average 177° for both compounds). The M–C_t (t = terminal) separations fall in the usual range found in other hexanuclear iridium

Table V.[a] **Relevant Spectroscopic and Structural Data for Selected Monoanionic Hexanuclear Iridium Clusters in Assigning the Bridging Character of Carbonyls**

		IR soln $\nu_{CO,b}$, cm^{-1}	NMR soln $\delta(^{13}C)$, ppm	Ir–C_b, Å		
				d_{min}	d_{max}	d_{av}
$[Ir_6(\mu_3\text{-}CO)_3(CO)_{12}(HgCl)]^-$	μ_3	1765	218.2	2.06	2.36	2.22
$[Ir_6(\mu\text{-}CO)_3(CO)_{12}\{Au(PPh_3)\}]^-$	μ	1790	208.5	2.06	2.13	2.10
$[Ir_6(\mu\text{-}CO)_2(CO)_{12}X]^{-\,b,c}$	μ	1815–1835		2.03	2.10	2.08
$[Ir_6(\mu_3\text{-}CO)_3(\mu\text{-}CO)(CO)_{11}X]^{-\,c}$	μ	1815		2.06	2.21	2.13
	μ_3	1787		2.08	2.41	2.22

[a] Metal–carbon bonding interactions are considered to be present if M–C distances are lower than 2.45 Å. [b] (X = Br, I) ref 8. [c] (X = Cl) ref 9.

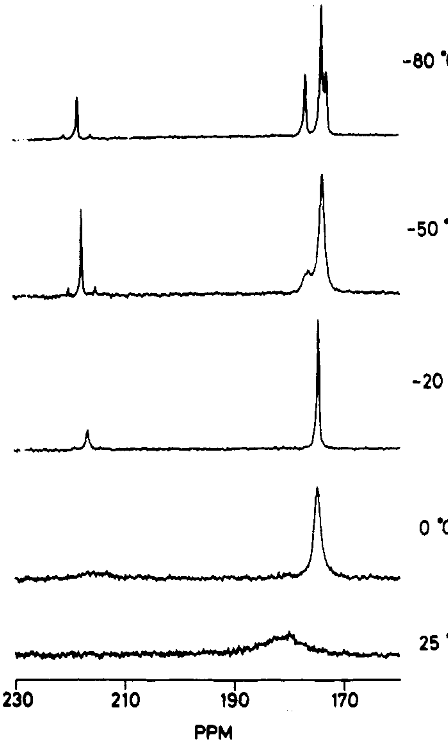

Figure 4. Variable-temperature ^{13}C NMR spectrum of $[N(PPh_3)_2][Ir_6(CO)_{15}(HgCl)]$. Temperature is indicated on the right in °C.

---

(14) See for example: (a) Fahmy, R.; King, K.; Rosenberg, E.; Tiripicchio, A.; Tiripicchio, Camellini, M. *J. Am. Chem. Soc.* **1980**, *102*, 3626. (b) Rosemberg, E.; Rychman, D.; Gellert, R. W.; Hsu, I. *Inorg. Chem.* **1986**, *25*, 195. (c) Iggo, J. A.; Mays, M. J. J. *J. Chem. Soc., Dalton Trans.* **1984**, 643. (d) Rosemberg, E.; Wang, J.; Gellert, R. W. *Organometallics* **1988**, *7*, 1093. (e) Braunstein, P.; Rosé, J.; Tiripicchio, A.; Tiripicchio Camellini, M. *Angew. Chem., Int. Ed. Engl.* **1985**, *24*, 767. (f) Yamamoto, Y.; Yamazaki, H.; Sakurai, T. *J. Am. Chem. Soc.* **1982**, *104*, 2329. (g) Albinati, A.; Moor, A.; Pregosin, P. S.; Venanzi, L. M. *J. Am. Chem. Soc.* **1982**, *104*, 7672. (h) Ermer, S.; King, K.; Hardcastle, K. I.; Rosenberg, E.; Manotti Lanfredi, A. M.; Tiripicchio, A.; Tiripicchio Camellini, M.; *Inorg. Chem.* **1983**, *22*, 1339. (i) Hajela, S.; Rosenberg, E.; Gobetto, R.; Milone, L.; Osella, D. *J. Organomet. Chem.* **1989**, *377*, 85 and references therein. (j) Bailey, P. J.; Johnson, B. F. G.; Lewis, J.; McPartlin, M.; Powell, H. R. *J. Chem. Soc., Chem. Commun.* **1989**, 1513. (k) Ragosta, J. M.; Burlitch, J. M. *Organometallics* **1988**, *7*, 1469. (l) Bailey, P. J.; Johnson, B. F. G.; Lewis, J.; McPartlin, M.; Powell, H. R. *J. Chem. Soc., Chem. Commun.* **1990**, 113. (m) Gade, L. H.; Johnson, B. F. G.; Lewis, J.; McPartlin, M.; Powell, H. R. H. *J. Chem. Soc. Chem. Commun.* **1990**, 110.

(15) For recent work see for example: (a) Henly, T. J.; Shapley, J. R. *Organometallics* **1989**, *8*, 2729. (b) Mednikov, E. G.; Basshilov, V. V.; Sokolov, V. I.; Slovokhotov, Y. L.; Struchkov, Y. T. *Polyhedron* **1983**, *2*, 141. (c) Braunstein, P.; Rosé, J.; Tiripicchio, A.; Tiripicchio Camellini, M. *J. Chem. Soc., Chem. Commun.* **1984**, 391. (d) Horwitz, C. P.; Holt, E. M.; Brock, C. P.; Shriver, D. F. *J. Am. Chem. Soc.* **1985**, *107*, 8136. (e) Henly, T. J.; Shapley, J. R. *Organometallics* **1989**, *8*, 2729.

(16) See for example: (a) Braunstein, P.; *New J. Chem.* **1986**, *10*, 365. (b) Raithby, P. R. In *Transition Metal Clusters*; Johnson, B. F. G., Ed.; Wiley: New York, 1980. (c) Gladfelter, W. L.; Geoffroy, G. L. *Adv. Organomet. Chem.* **1980**, *18*, 207. (d) Farrar, D. H.; Goudsmit, R. J. In *Metal Clusters*; Moskovits, M., Ed.; Wiley: New York, 1986.

(17) See for example: (a) Johnson, B. F. G.; Kaner, D. A.; Lewis, J.; Raithby, P. R. *J. Organomet. Chem.* **1981**, *215*, C33. (b) Johnson, B. F. G.; Lewis, J.; Raithby, P. R.; Taylor, M. J. *J. Chem. Soc., Chem. Commun.* **1982**, 314. (c) Mays, M. J.; Raithby, P. R.; Taylor, P. L.; Henrick, K. J. *Organomet. Chem.* **1982**, *224*, C45. (d) Green, M.; Mead, K. A.; Mills, R. M.; Salter, I. D.; Stone; F. G. A.; *J. Chem. Soc., Chem. Commun.* **1982**, 51. (e) Bateman, L. W.; Green, M.; Howard, J. A. K.; Mead, K. A.; Mills, R. M.; Salter, I. D.; Stone, F. G. A.; Woodward, P. *J. Chem. Soc., Chem. Commun.* **1982**, 773.

(18) Braga, D.; Grepioni, F. *J. Organomet. Chem.* **1987**, *336*, C9.

(19) (a) Lehner, H.; Matt, D.; Pregosin, P. S.; Venanzi, L. M.; Albinati, A. *J. Am. Chem. Soc.* **1982**, *104*, 6825. (b) Casalnuovo, A. L.; Pignolet, L. H.; Van der Velden, J. W. A.; Bour, J. J.; Steggerda, J. J. *J. Am. Chem. Soc.* **1983**, *105*, 5957. (c) Casalnuovo, A. L.; Laska, T.; Nilsson, P. V.; Olofson, J.; Pignolet, L. H.; Bos, W.; Bour, J. J.; Steggerda, J. J. *Inorg. Chem.* **1985**, *24*, 182. (d) Casalnuovo, A. L.; Laska, T.; Nilsson, P. V.; Olofson, J.; Pignolet, L. H. *Inorg. Chem.* **1985**, *24*, 233. (e) Casalnuovo, A. L.; Casalnuovo, J. A.; Nilsson, P. V.; Pignolet, L. H. *Inorg. Chem.* **1985**, *24*, 2554. (f) Alexander, B. D.; Johnson, B. J.; Johnson, S. M.; Casalnuovo, A. L.; Pignolet, L. H. *J. Am. Chem. Soc.* **1986**, *108*, 4409. (g) Nicholls, J. N.; Raithby, P. R.; Vargas, M. D. *J. Chem. Soc., Chem. Commun.* **1986**, 1617.

(20) (a) Brotherton, P. D.; Raston, C. L.; White, A. H.; Wild, S. B. *J. Chem. Soc., Dalton Trans.* **1976**, 1799. (b) van Vliet, P. I.; Kokkes, M.; van Koten, G.; Vrieze, K. *J. Organomet. Chem.* **1980**, *187*, 413.

carbonyl clusters (average Ir–C 1.86 Å for 1, 1.87 Å for 2).[3-10] The coordination of the bridging carbonyl ligands is slightly different in 1 and 2, where three face- and three edge-bridging CO groups are present, respectively. A slight bending of the μ-carbonyls is however present in 2, generating "semitriple" bridging carbonyls. Considering the longest Ir–C_b (b = bridging) bond distance in 1, 2.36 (2) Å, and the shortest nonbonding Ir···C_b contact, 2.60 (2) Å, in 2, we conclude that the carbonyl topology is, at least in the solid state, different in 1 and 2 and in agrement with the IR spectra in solution (see Table V). Therefore, the anion 1 possesses idealized C_{3v} symmetry, while 2 belongs to the C_3 idealized point group. Bond parameters for the face-bridging carbonyl groups in 1 range from 2.04 (2) to 2.36 (2) Å with an average value of 2.22 Å, whereas for the edge-bridging ligands in 2 they are essentially equal [range 2.06 (1)–2.11 (1) Å], with an average value of 2.10 Å. The resulting disposition of the bridging carbonyl groups relates 2 to the dianion $[Ir_6(CO)_{15}]^{2-}$,[10,21] which keeps unchanged the ligands assembly after the reaction with the $[Au(PPh_3)]^+$ cation, and relates 1 to the red isomer of $Ir_6(CO)_{16}$, by replacement of a μ_3-CO with the μ_3-HgCl group. This difference might be surprising since $[Au(PPh_3)]^+$ and $[HgCl]^+$ are isoelectronic groups, although sterically different. However, if we consider complex 1 as being formed from a Cl^-, Hg(0), and an Ir_6 neutral fragment, we can postulate a weak electron donor ability of the $[HgCl]^-$ fragment, formally comparable to that of CO. On the contrary such a distribution of formal oxidation numbers in 2 would imply an unreasonable $[Au(PPh_3)]^-$ group and therefore must be ruled out.

NMR Studies. The numbering scheme for labeling the carbon atoms in the NMR spectra is the same as that used in the crystallographic study. The ^{13}C NMR spectra of complexes 1 and 2 were recorded both in CD_2Cl_2 and THF-d_8: the best resolution was obtained in dichloromethane for 1 and in THF for 2. ^{13}C NMR spectra for $[Ir_6(CO)_{15}(HgCl)]^-$ and for $[Ir_6(CO)_{15}[Au(PPh_3)]]^-$ at several temperatures are shown in Figures 4 and 5, respectively.

$[Ir_6(CO)_{15}(HgCl)]^-$. The number of signals of the ^{13}C NMR spectrum, at low temperature, is entirely in agreement with the structure shown in Figure 1. Thus, the limiting low-temperature ^{13}C NMR spectrum at −80 °C shows four signals. Three resonances at δ 173.0, 173.8, and 176.8 ppm, in the ratio 1:2:1, can be assigned to three inequivalent groups of terminal carbonyls. The signal at δ 173.8 ppm is due to six equivalent carbonyl ligands [C(11), C(12), C(21), C(22), C(31), and C(32)]. The remaining two equally intense signals are due to axial and radial carbonyl groups.[22] The resonances at δ 173.0 and 176.8 ppm cannot be assigned with certainty, but by analogy with that found in the ^{13}C NMR studies on tetranuclear iridium carbonyl clusters,[23] we attribute the signal at higher field to the axial ligands [C(42), C(52), and C(62)] and the signal at δ 176.8 ppm to carbon atoms C(41), C(51), and C(61). The fourth signal, of relative intensity 1, at δ 218.2 ppm is assigned to the face-bridging carbonyl ligands [CT(1), CT(2), and CT(3)], because of the low-field position and of the presence of the mercury satellites [$^2J(^{199}Hg-^{13}C)$ = 248 Hz].

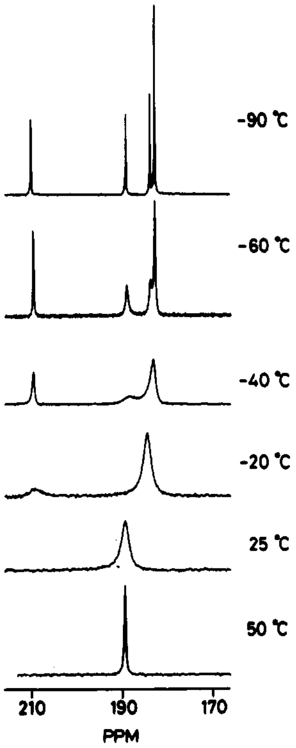

Figure 5. Variable-temperature ^{13}C NMR spectrum of $[N(PPh_3)_2][Ir_6(CO)_{15}[Au(PPh_3)]]$. Temperature is indicated on the right in °C.

Variable-temperature experiments (Figure 4) show that all the terminal carbonyl ligands start to average simultaneously at about −50 °C, when their resonances broaden significantly, whereas the face-bridging carbonyl groups produce a sharp signal. The terminal CO ligands become equivalent, on the NMR time scale, at −20 °C, and the three resonances collapse to a single line at δ 174.6 ppm (calculated average value 174.4 ppm). At higher temperature, a second averaging process can be observed: at 0 °C, the signals due to terminal and bridging carbonyls collapse. At room temperature a single, very broad signal can be observed at δ 182.3 ppm (calculated mean value 183.1 ppm). This peak sharpens with increasing temperature, and at 70 °C (THF-d_8) the signal is quite narrow, suggesting a complete scrambling of all the 15 carbonyl ligands over the octahedron framework of 1, but the expected satellites with Hg (calculated average J value = 49 Hz) can not be detected, probably because the spectrum is not limiting.

For anion 1, the ^{199}Hg NMR spectrum (THF-d_8), at −98 °C, shows a signal at δ −1168 ppm (see later).

$[Ir_6(CO)_{15}[Au(PPh_3)]]^-$. In 2, the presence of formal edge-bridging ligands lowers the symmetry of the anion to C_3 and the mirror planes present in 1 are lost; thus, the six carbonyls bonded to the iridium atoms bonded to gold should be split into two sets of three equivalent ligands. Therefore, the full spectrum should show five equally intense peaks. Instead, the ^{13}C spectrum (THF-d_8) of 2 at −80 °C contains only four signals: three in the terminal carbonyl region at δ 180.8, 181.9, and 187.3 ppm of intensity 2:1:1, and one at δ 208.5 ppm, of intensity 1, associated with the edge-bridging CO groups. The coincidence of two

---

[21] The structure of the $[Ir_6(CO)_{15}]^{2-}$ dianion consists of an essentially regular octahedron of metal atoms connected to twelve terminal and three symmetrically edge-bridging carbonyl ligands. All the iridium atoms bind one edge-bridging and two terminal carbonyl groups, so that the overall idealized symmetry of the anion is D_3.[10]

[22] For 1 and 2 we consider axial carbonyl groups the ligands perpendicular to the face defined by Ir(4), Ir(5), and Ir(6); the remaining carbonyl ligands, which are almost coplanar to the same face, are considered radial.

[23] (a) Stuntz, G. F.; Shapley, J. R. *J. Am. Chem. Soc.* **1977**, *99*, 607. (b) Shapley, J. R.; Stuntz, G. F. *J. Chem. Soc., Chem. Commun.* **1979**, 219. (c) Stuntz, G. F.; Shapley, J. R. *J. Organomet. Chem.* **1981**, *213*, 389. (d) Mann, B. E.; Spencer, C. M. *J. Organomet. Chem.* **1983**, *244*, C17. (e) Strawczynski, A.; Ros, R.; Roulet, R. *Helv. Chim. Acta* **1988**, *71*, 867. (f) Strawczynski, A.; Ros, R.; Roulet, R.; Grepioni, F.; Braga, D. *Helv. Chim. Acta* **1988**, *71*, 1885.

signals, in the terminal CO region, can be due (i) to the essential similarity, from the NMR point of view, of the carbonyl groups of the capped face or (ii) to the presence of two equivalent energetic minima corresponding to the two enantiomeric C_3 structures (separated by a μ_3-CO low-energy hill), therefore mimicking, on the NMR time scale, statistical idealized C_{3v} symmetry. On the basis of chemical shifts, of the intensities of the signals and of the relative position of the axial and radial CO, we assign the resonance at δ 180.8 ppm to CO groups [C(11), C(12), C(21), C(22), C(31), and C(32)], the resonance at δ 181.9 ppm, to the axial CO[22] ligands [(C(42), C(52), and C(62)], and finally the last signal, to the radial[22] CO ligands [C(41), C(51), and C(61)]. Further support for the assignment of the resonance at δ 208.5 ppm to bridging ligands comes from the phosphorus carbon coupling [$^3J(^{31}P-^{13}C)$ = 7.7 Hz]. The variable-temperature spectra indicate (Figure 5) that a low-energy process occurs at −60 °C, causing only the broadening of the resonances of the terminal carbonyls. This process is the only one occurring to an appreciable extent, on the NMR time scale, over the temperature range −60 to −40 °C; at the latter temperature the bridging ligands become fluxional. At −20 °C only two broad signals, at δ 182.7 ppm (average value 182.7 ppm) and at δ 207.1 ppm, can be observed. Only one signal at δ 187.6 ppm (mean 187.8 ppm) is present at room temperature, but it becomes sharp only at 50 °C.

The $^{31}P\{^1H\}$ NMR spectrum of 2, in THF-d_8, at −68 °C shows, as expected, a sharp singlet at δ 98.5 ppm (see later).

The variable-temperature experiments suggest that both 1 and 2 undergo two distinct fluxional processes: the first process, which occurs at lower temperatures, averages only the terminal ligands, and the second, which takes place at higher temperatures, involves also the bridging CO ligands. In 1 the two phenomena happen at two well-separated temperatures, whereas in 2 they are almost simultaneous because the μ-CO are more mobile at lower temperatures than the μ_3-CO ligands.

The two low-energy processes can be accounted for by two distinct mechanisms: (i) a merry-go-round[24] movement of the terminal ligands around the bridged faces, which can be proposed because the ligands are almost coplanar with the right disposition for a such migration, (ii) dissociation of the HgCl$^+$ or [Au(PPh$_3$)]$^+$ group, with the intermediate formation of $[Ir_6(CO)_{15}]^{2-}$, and capping of the opposite triangular face. The first process, i.e. the concerted scrambling of six terminal ligands around the triangular faces, observed in $Ir_4(CO)_{11}(CNBu^t)$,[23c] seems unlikely in our case owing to the presence of the bulky bridging groups. Therefore we devised NMR experiments that could prove the existence of the second process.

Thus, we registered the NMR spectra of ^{199}Hg for 1 and ^{31}P for 2, at several temperatures, both in the presence and in the absence of the excess HgCl$_2$ and Au(PPh$_3$)Cl, respectively.

As already mentioned, the ^{199}Hg NMR spectrum of 1 shows, at low temperature, a signal at δ −1168 ppm but this resonance disappears at room temperature. The results of the experiments carried out in the presence of HgCl$_2$ could not be simply explained. However, the experiments support the idea that a fast intermolecular exchange takes place in the whole range of temperatures. This fact, associated with the coupling with quadrupolar nuclei of iridium and chlorine can also explain the disappearance of the ^{199}Hg signal at room temperature.

Table VI. Crystal Data and Data Collection Parameters

compd	**1a**	**2a**
formula	$C_{54}H_{36}ClHgIr_6NO_{15}P_2$	$C_{47}H_{39}AuIr_6NO_{16}P$
fw	2390.08	2254.97
cryst syst	triclinic	triclinic
space group	$P\bar{1}$	$P\bar{1}$
a, Å	14.115 (5)	13.582 (2)
b, Å	14.619 (3)	14.513 (2)
c, Å	17.762 (5)	14.624 (4)
α, deg	71.21 (2)	110.07 (2)
β, deg	66.43 (2)	91.75 (2)
γ, deg	64.61 (2)	98.37 (1)
V, Å^3	2984 (1)	2669 (2)
Z	2	2
D_{calcd}, g cm^{-3}	2.660	2.806
μ(Mo Kα), cm^{-1}	159.99	176.74
min transm fact.	0.41	0.51
scan mode	ω	ω
ω-scan width, deg	1.2 + 0.35 tan θ	1.2 + 0.35 tan θ
θ range, deg	3–25	3–25
octants of reciprocal space explored	$\pm h,\pm k,+l$	$\pm h,\pm k,+l$
measd reflns	10 549	9342
unique obsd reflns with $I > 3\sigma(I)$	4513	6011
final R and R_w[a]	0.039, 0.044	0.033, 0.043
no. of variables	521	479
GOF[b]	1.382	1.274

[a] $R = [\sum(F_o - k|F_c|)/\sum F_o]$ and $R_w = [\sum w(F_o - k|F_c|)^2/\sum wF_o^2]^{1/2}$. [b] $GOF = [\sum w(F_o - k|F_c|)^2/(N(\text{observations}) - N(\text{variables}))]^{1/2}$.

As reported above, in the case of complex 2 the ^{31}P NMR spectrum shows a single signal and this resonance is not affected either by the temperature variation or by addition of Au(PPh$_3$)Cl. We also added a catalytic amount of the solvated cation [Au(PPh$_3$)]$^+$, but in this case a small signal due to a new species was observed. We can therefore exclude a dissociation of 2, but an intramolecular migration can still be postulated.

It must be noted that the ^{13}C spectra of the two compounds at −80 °C are perfectly consistent with the 3-fold symmetry of the compounds found in the solid state but are not a conclusive proof that the two clusters adopt in solution different ligand arrangements. Thus, the two low-field resonances due to μ_3-CO in 1 and μ-CO in 2 lie very close to each other with only 10 ppm difference between their chemical shifts. This observation alone cannot aid us to assign unambiguously the two structures in solution and is directly related to the earlier observations[25] of ^{13}C chemical shifts, where the resonances of carbonyl groups follow the sequence *terminal* < *edge bridging* < *face bridging* and are well separated. The spectroscopic and structural data of 1 and 2, which are the most relevant in assigning the bridging character of carbonyls, are reported in Table V. We finally assign to the mercury derivative a C_{3v} structure both in the solid state and in solution. The small differences observed between the tabulated parameters of compounds 1a and 2a and the comparison to the known literature data summarized in Table V, however, suggest a C_3 rather than C_{3v} idealized symmetry for 2, with slight bending of the μ-bridging CO groups toward a "semitriple" coordination.

Experimental Section

All operations were carried out under nitrogen atmosphere with the use of standard Schlenk-tube and vacuum line techniques.[26]

---

(24) (a) Cotton, F. A.; Kruczynski, L.; Shapiro, B. L.; Johnson, L. F. *J. Am. Chem. Soc.* **1972**, *94*, 6191. (b) Cotton, F. A. *Inorg. Chem.* **1966**, *5*, 1083.

(25) (a) Chini, P.; Martinengo, S.; McCaffrey, J. A.; Heaton, B. T. H. *J. Chem. Soc., Chem. Commun.* **1974**, 310. (b) Heaton, B. T. H.; Towl, A. D. C.; Chini, P.; Fumagalli, A.; McCaffrey, J. A.; Martinengo, S. *J. Chem. Soc., Chem. Commun.* **1975**, 523.

Table VII. Fractional Atomic Coordinates for $[N(PPh_3)_2][Ir_6(CO)_{15}(HgCl)]\bullet 0.5C_6H_{12}$ (1a) with Esd's in Parentheses[a]

atom	*x*	*y*	*z*	atom	*x*	*y*	*z*
Hg	0.16725 (6)	0.24046 (6)	−0.05058 (4)	CT(3)	0.081 (1)	0.278 (1)	0.234 (1)
Ir(1)	0.06368 (5)	0.11801 (5)	0.08561 (4)	C(111)	0.275 (1)	0.217 (1)	0.4599 (9)
Ir(2)	0.28845 (5)	0.09719 (5)	0.05465 (4)	C(112)	0.274 (2)	0.140 (1)	0.531 (1)
Ir(3)	0.11093 (5)	0.27914 (5)	0.10885 (4)	C(113)	0.180 (2)	0.111 (1)	0.571 (1)
Ir(4)	0.01291 (6)	0.15460 (6)	0.24313 (5)	C(114)	0.095 (2)	0.158 (1)	0.540 (1)
Ir(5)	0.18326 (6)	−0.02112 (5)	0.19042 (4)	C(115)	0.094 (2)	0.231 (2)	0.474 (1)
Ir(6)	0.22971 (5)	0.13277 (5)	0.21288 (3)	C(116)	0.186 (1)	0.265 (1)	0.429 (1)
Cl	0.1884 (5)	0.3074 (6)	−0.1931 (4)	C(121)	0.491 (1)	0.165 (1)	0.3345 (9)
P(1)	0.3966 (3)	0.2517 (3)	0.4031 (3)	C(122)	0.497 (1)	0.061 (1)	0.356 (1)
P(2)	0.3189 (3)	0.4796 (3)	0.3543 (3)	C(123)	0.582 (2)	−0.009 (1)	0.300 (1)
O(11)	−0.150 (1)	0.259 (1)	0.051 (1)	C(124)	0.658 (2)	0.023 (2)	0.237 (1)
O(12)	0.1264 (9)	−0.0190 (9)	−0.0343 (7)	C(125)	0.651 (2)	0.120 (2)	0.214 (1)
O(21)	0.3883 (9)	−0.0485 (9)	−0.0661 (7)	C(126)	0.566 (1)	0.192 (1)	0.265 (1)
O(22)	0.4523 (9)	0.2082 (9)	−0.0300 (7)	C(131)	0.465 (1)	0.235 (1)	0.4766 (9)
O(31)	0.246 (1)	0.4188 (9)	0.0294 (9)	C(132)	0.576 (1)	0.200 (1)	0.458 (1)
O(32)	−0.097 (1)	0.453 (1)	0.086 (1)	C(133)	0.625 (2)	0.200 (2)	0.512 (1)
O(41)	−0.224 (1)	0.282 (1)	0.263 (1)	C(134)	0.564 (1)	0.234 (1)	0.584 (1)
O(42)	−0.036 (1)	0.082 (1)	0.4276 (8)	C(135)	0.453 (1)	0.269 (1)	0.604 (1)
O(51)	0.264 (1)	−0.2005 (9)	0.1060 (8)	C(136)	0.401 (1)	0.273 (1)	0.552 (1)
O(52)	0.181 (1)	−0.150 (1)	0.3618 (7)	C(211)	0.213 (1)	0.547 (1)	0.3070 (9)
O(61)	0.3812 (9)	0.2458 (9)	0.1758 (8)	C(212)	0.215 (2)	0.513 (1)	0.242 (1)
O(62)	0.247 (1)	0.0217 (9)	0.3850 (7)	C(213)	0.133 (2)	0.571 (2)	0.201 (1)
OT(1)	−0.0571 (9)	−0.0190 (8)	0.2229 (7)	C(214)	0.057 (2)	0.660 (2)	0.222 (1)
OT(2)	0.4398 (8)	−0.0589 (8)	0.1547 (6)	C(215)	0.050 (2)	0.695 (2)	0.288 (1)
OT(3)	0.053 (1)	0.3408 (8)	0.2753 (7)	C(216)	0.130 (1)	0.639 (1)	0.330 (1)
N	0.3694 (9)	0.3606 (9)	0.3477 (7)	C(221)	0.422 (1)	0.537 (1)	0.2982 (8)
C(11)	−0.067 (2)	0.205 (1)	0.063 (1)	C(222)	0.532 (1)	0.481 (1)	0.284 (1)
C(12)	0.105 (1)	0.033 (1)	0.0091 (9)	C(223)	0.610 (2)	0.527 (1)	0.240 (1)
C(21)	0.350 (1)	0.010 (1)	−0.0214 (9)	C(224)	0.578 (1)	0.631 (1)	0.209 (1)
C(22)	0.387 (1)	0.166 (1)	0.0022 (9)	C(225)	0.475 (1)	0.686 (1)	0.223 (1)
C(31)	0.194 (1)	0.367 (1)	0.060 (1)	C(226)	0.390 (1)	0.645 (1)	0.265 (1)
C(32)	−0.015 (2)	0.382 (1)	0.093 (1)	C(231)	0.264 (1)	0.507 (1)	0.459 (1)
C(41)	−0.129 (2)	0.231 (2)	0.254 (1)	C(232)	0.321 (1)	0.540 (1)	0.487 (1)
C(42)	−0.020 (1)	0.110 (1)	0.357 (1)	C(233)	0.281 (2)	0.550 (2)	0.571 (1)
C(51)	0.234 (1)	−0.134 (1)	0.140 (1)	C(234)	0.187 (2)	0.532 (2)	0.622 (1)
C(52)	0.182 (1)	−0.100 (1)	0.2977 (9)	C(235)	0.132 (2)	0.499 (2)	0.594 (1)
C(61)	0.326 (1)	0.201 (1)	0.1925 (9)	C(236)	0.167 (1)	0.486 (1)	0.513 (1)
C(62)	0.243 (1)	0.068 (1)	0.320 (1)	CS(1)	0.476 (2)	0.553 (2)	0.060 (2)
CT(1)	0.006 (1)	0.024 (1)	0.197 (1)	CS(2)	0.516 (3)	0.443 (3)	0.080 (2)
CT(2)	0.355 (1)	0.000 (1)	0.1487 (9)	CS(3)	0.572 (3)	0.398 (3)	0.011 (2)

[a] Abbreviations for atoms in Tables VII and VIII: CS = carbon of solvent molecule; OS = oxygen of solvent molecule.

Reaction solvents were purified and dried by distillation, immediately before use, under nitrogen atmosphere from the following solvent/drier combinations: THF/Na–benzophenone ketyl; C_6H_{12}/Na; CH_2Cl_2/P_2O_5; $Pr^iOH/[Al(OPr^i)_3]$.

Infrared spectra (IR) were recorded on a Perkin-Elmer 781 grating spectrophotometer using 0.1-mm calcium fluoride cells previously purged with nitrogen. Variable-temperature $^{13}C\{^1H\}$ NMR spectra were recorded at 50.3 MHz on a Bruker AC200 spectrometer and are reported in ppm downfield from the external standard $SiMe_4$. $^{31}P\{^1H\}$ and $^{199}Hg\{^1H\}$ NMR spectra were recorded on a Bruker AC200 spectrometer, operating at 81.0 MHz for phosphorus and at 35.76 MHz for mercury (pulse repetition rate 1.2 s, and 90° pulse, 10 μs) and are reported in ppm downfield from the external standard (85% H_3PO_4 in D_2O for phosphorus, $HgMe_2$ for mercury).

$[N(PPh_3)_2]_2[Ir_6(CO)_{15}]$ and $[NMe_3(CH_2Ph)]_2[Ir_6(CO)_{15}]$ were prepared by literature methods.[2b,10] ^{13}CO-enriched samples of $[N(PPh_3)_2]_2[Ir_6(^{13}CO)_{15}]$ (ca. 20–30%) were obtained by reacting enriched $[N(PPh_3)_2][Ir(^{13}CO)_4]$ with $Ir_4(CO)_{12}$.[2b]

Samples for mass spectrometry were suspended in a matrix of *m*-nitrobenzyl alcohol/sulfolane and bombarded with a beam of xenon atoms at 70 keV with a VG Micromass 7600 machine; spectra were obtained by the staff of the Laboratorio Analisi Universitá di Milano. Theoretical isotope patterns were calculated with the aid of the computer program ISO provided by the manufacturer. Calibration was checked before acquisition of data by using the reference spectrum of CsI clusters. Matrix additions are well-known in FAB mass spectra and did not lead to significant complications with the clusters studied here.[27]

Elemental analyses were performed by the Microanalytical Laboratory of Dipartimento di Chimica Inorganica e Metallorganica at University of Milano.

Preparation of $[N(PPh_3)_2][Ir_6(CO)_{15}(HgCl)]$ (1a). Addition of 0.076 g (0.28 mmol) of $HgCl_2$ to a solution of $[N(PPh_3)_2]_2[Ir_6(CO)_{15}]$ (0.712 g, 0.27 mmol) in 30 mL of THF causes a color change from dark brown-red to deep red. The mixture was stirred at room temperature for 30 min, and the completeness of the reaction was checked by IR spectroscopy, which showed only the formation of $[Ir_6(CO)_{15}(HgCl)]^-$. The solution was filtered, and the product was recovered by adding cyclohexane (30 mL) and removing partially the solvent by vacuum distillation. The dark red precipitate was filtered off, washed with 2-propanol (3 × 10 mL) and hexane (3 × 10 mL), and dried. Yield: 0.431 g (68%). Slow diffusion of cyclohexane (30 mL) cautiously layered on a solution of the product in THF (15 mL) gave prismatic crystals of $[N(PPh_3)_2][Ir_6(CO)_{15}(HgCl)]\cdot 0.5C_6H_{12}$. Elemental analysis is in agreement with a cluster unit containing half a molecule of clathrated cyclohexane, as confirmed by the ^1H NMR (acetone-d_6) spectrum of selected single crystals. Anal. Calcd for $C_{54}H_{36}ClHgIr_6NO_{15}P_2$: C, 27.14; H, 1.51; N, 0.59. Found: C, 27.02; H, 1.42; N, 0.51.

It should be noted that prolonged vacuum drying or very long exposure to the air can remove some clathrated C_6H_{12}.

FAB-MS (negative ions): The observed spectrum has two overlapping fragmentation processes. First process, *m/z*: 1813 (^{193}Ir, ^{200}Hg, ^{35}Cl), $[M]^-$; 1785, 1757, 1729, $[M]^- - xCO$ ($x = 1$–3); 1529, $[M]^- - 3CO - Hg$; 1501, 1473, 1445, 1417, $[M]^- - Hg - xCO$ ($x = 4$–7). Second process, *m/z*: 1578, $[M]^- - HgCl$; 1550, 1522,

---

(26) Shriver, D. F.; Drezdzon, M. A. In *The Manipulation of Air-sensitive Compounds*, 2nd ed.; Wiley: New York, 1986.

(27) (a) Miller, J. M. *J. Organomet. Chem.* **1983**, *249*, 299. (b) Grover, J. L. *Biomed. Mass Spectrom.* **1985**, *12*, 191. (c) Sharp, T. R.; White, M. R.; Davis, J. F.; Stang, P. J. *J. Org. Mass Spectrom.* **1984**, *19*, 107.

Table VIII. Fractional Atomic Coordinates for $[NMe_3(CH_2Ph)][Ir_6(CO)_{15}[Au(PPh_3)]]\bullet C_4H_8O$ (2a) with Esd's in Parentheses

atom	*x*	*y*	*z*	atom	*x*	*y*	*z*
Au	0.21436 (3)	−0.01962 (4)	0.25281 (3)	CD(1)	−0.0861 (9)	−0.1575 (9)	0.0296 (9)
Ir(1)	0.03624 (3)	−0.08524 (3)	0.12807 (3)	CD(2)	0.057 (1)	−0.3708 (9)	0.154 (1)
Ir(2)	0.13193 (3)	−0.22555 (3)	0.18224 (3)	CD(3)	−0.1102 (8)	−0.1280 (9)	0.3505 (9)
Ir(3)	0.03417 (3)	−0.08723 (3)	0.32229 (3)	C(111)	0.4631 (8)	0.0148 (9)	0.3221 (8)
Ir(4)	−0.13804 (3)	−0.15131 (3)	0.20097 (3)	C(112)	0.462 (1)	−0.083 (1)	0.265 (1)
Ir(5)	−0.04388 (3)	−0.28177 (4)	0.05736 (4)	C(113)	0.533 (1)	−0.134 (1)	0.286 (1)
Ir(6)	−0.04372 (4)	−0.29182 (4)	0.24418 (4)	C(114)	0.603 (1)	−0.087 (1)	0.366 (1)
P	0.3682 (2)	0.0761 (2)	0.2868 (2)	C(115)	0.603 (1)	0.006 (1)	0.421 (1)
O(11)	0.0020 (8)	0.1284 (6)	0.1858 (7)	C(116)	0.534 (1)	0.064 (1)	0.404 (1)
O(12)	0.1822 (7)	−0.0804 (7)	−0.0236 (7)	C(121)	0.4174 (9)	0.1038 (9)	0.1832 (9)
O(21)	0.2812 (7)	−0.2599 (9)	0.0301 (8)	C(122)	0.520 (1)	0.111 (1)	0.169 (1)
O(22)	0.2785 (7)	−0.2290 (9)	0.3366 (8)	C(123)	0.548 (1)	0.134 (1)	0.086 (1)
O(31)	0.1504 (7)	−0.1006 (7)	0.4952 (7)	C(124)	0.484 (1)	0.148 (1)	0.023 (1)
O(32)	0.0450 (7)	0.1339 (6)	0.4013 (7)	C(125)	0.385 (1)	0.141 (1)	0.038 (1)
O(41)	−0.2258 (8)	0.0351 (7)	0.2295 (9)	C(126)	0.354 (1)	0.118 (1)	0.118 (1)
O(42)	−0.3371 (7)	−0.2829 (9)	0.1339 (9)	C(131)	0.3809 (9)	0.1944 (9)	0.3865 (9)
O(51)	0.0727 (8)	−0.356 (1)	−0.1169 (7)	C(132)	0.459 (1)	0.276 (1)	0.394 (1)
O(52)	−0.2284 (8)	−0.4368 (9)	−0.0230 (9)	C(133)	0.473 (1)	0.359 (1)	0.478 (1)
O(61)	0.0118 (9)	−0.3232 (8)	0.4298 (7)	C(134)	0.408 (1)	0.366 (1)	0.552 (1)
O(62)	−0.2296 (9)	−0.4464 (9)	0.202 (1)	C(135)	0.335 (1)	0.291 (1)	0.543 (1)
OD(1)	−0.1357 (7)	−0.1466 (7)	−0.0310 (6)	C(136)	0.319 (1)	0.206 (1)	0.4622 (9)
OD(2)	0.0738 (7)	−0.4492 (6)	0.1276 (8)	C(211)	0.136 (2)	0.480 (2)	0.293 (2)
OD(3)	−0.1587 (6)	−0.1225 (6)	0.4166 (6)	C(212)	0.196 (1)	0.318 (1)	0.256 (1)
N	0.1651 (9)	0.4041 (9)	0.3330 (9)	C(213)	0.079 (2)	0.366 (2)	0.381 (2)
C(11)	0.0179 (9)	0.0494 (9)	0.1626 (8)	C(214)	0.254 (1)	0.456 (1)	0.409 (1)
C(12)	0.1288 (8)	−0.0796 (9)	0.0382 (8)	C(215)	0.237 (1)	0.543 (1)	0.499 (1)
C(21)	0.2260 (9)	−0.244 (1)	0.088 (1)	C(216)	0.253 (1)	0.639 (1)	0.500 (1)
C(22)	0.2246 (9)	−0.224 (1)	0.280 (1)	C(217)	0.239 (1)	0.715 (1)	0.585 (1)
C(31)	0.1080 (9)	−0.0929 (9)	0.431 (1)	C(218)	0.217 (2)	0.701 (2)	0.668 (2)
C(32)	0.0428 (9)	0.0521 (9)	0.3724 (8)	C(219)	0.201 (2)	0.602 (2)	0.668 (1)
C(41)	−0.1919 (9)	−0.035 (1)	0.217 (1)	C(220)	0.211 (1)	0.528 (1)	0.584 (1)
C(42)	−0.2604 (9)	−0.2323 (9)	0.162 (1)	OS	0.414 (1)	0.477 (1)	0.250 (1)
C(51)	0.028 (1)	−0.329 (1)	−0.0495 (9)	CS(1)	0.419 (2)	0.568 (2)	0.220 (2)
C(52)	−0.156 (1)	−0.379 (1)	0.010 (1)	CS(2)	0.480 (2)	0.532 (2)	0.133 (2)
C(61)	−0.008 (1)	−0.3101 (9)	0.360 (1)	CS(3)	0.500 (2)	0.438 (2)	0.111 (2)
C(62)	−0.159 (1)	−0.388 (1)	0.218 (1)	CS(4)	0.483 (2)	0.408 (2)	0.198 (2)

1494, 1466, 1438, 1410, $[M]^- - HgCl - x CO$ (x = 1–6).

Preparation of $[NMe_3(CH_2Ph)][Ir_6(CO)_{15}[Au(PPh_3)]]$ (2a). A 0.012 M solution containing the cation $[Au(PPh_3)]^+$ was prepared by treating $Au(PPh_3)Cl$ (0.043 g, 0.087 mmol) with $Ag[BF_4]$ (0.015 g, 0.078 mmol) in THF (6.5 mL). This solution was added, in 2.5-mL portions, to a THF (10 mL) solution of $[NMe_3(CH_2Ph)]_2[Ir_6(CO)_{15}]$ (0.112 g, 0.06 mmol). The reaction mixture was checked by IR spectroscopy after each addition, and the reaction was complete after 5 mL; at the end the solution was dark red. The solution was filtered, concentrated in vacuum to about 4 mL, and then cyclohexane (40 mL) was added dropwise with stirring, causing precipitation of $[NMe_3(CH_2Ph)][Ir_6(CO)_{15}[Au(PPh_3)]]$ as a fine powder. The compound was collected by filtration, under inert atmosphere, washed with cyclohexane (3 × 10 mL), and vacuum-dried. Yield: 0.098 g (75%). Crystallization of **2a** from THF/cyclohexane layering yielded dark red crystals of $[NMe_3(CH_2Ph)][Ir_6(CO)_{15}[Au(PPh_3)]]{\cdot}C_4H_8O$. Elemental analysis is in agreement with a cluster unit containing a molecule of clathrated tetrahydrofuran.

Anal. Calcd for $C_{47}H_{39}AuIr_6NO_{16}P$: C, 25.03; H, 1.73; N, 0.62. Found: C, 25.22; H, 1.65; N, 0.41.

It should be noted that prolonged vacuum drying or very long exposure to the air xCO remove some clathrated C_4H_8O.

FAB-MS (negative ion), *m/z*: 2037 (^{193}Ir), $[M]^-$; 2009, 1981, 1953, 1925, 1897, $[M]^- - x CO$ (x = 1–5).

The $[N(PPh_3)_2]^+$ salt can be prepared in a similar way.

Reaction of $[N(PPh_3)_2][Ir_6(CO)_{15}(HgCl)]$ with I_2. $[N(PPh_3)_2][Ir_6(CO)_{15}(HgCl)]$ (0.338, 0.14 mmol) in THF (10 mL) was treated, while being stirred, with 2.4 mL of a 0.1 M solution of I_2 in THF. An immediate reaction was observed with color change to orange-brown while the IR spectrum showed quantitative formation of $[Ir_6(CO)_{15}I]^-$.

Reaction of $[N(PPh_3)_2][Ir_6(CO)_{15}[Au(PPh_3)]]$ with Cl^-. A solution of 2 (0.072 g, 0.028 mmol) in CH_2Cl_2 (5 mL) was reacted with $[N(PPh_3)_2]Cl$ (0.048 g, 0.084 mmol) at room temperature for 10 min. The characteristic strong carbonyl bands of $[Ir_6(CO)_{15}]^{2-}$ were immediately observed in the infrared spectrum of the product mixture.

Collection and Reduction of the X-ray Data for 1a and 2a. The crystal data for compounds **1a** and **2a** are summarized in Table VI together with some experimental details. Crystals of the two compounds were mounted in an arbitrary orientation on a glass fiber, which was then fixed into an aluminum pin and mounted onto a goniometer head. Diffraction data were collected on an Enraf-Nonius CAD4 automated diffractometer using Mo Kα radiation (λ = 0.71073 Å) with a graphite crystal monochromator in the incident beam. The Enraf-Nonius program SEARCH was employed to obtain 25 accurately centered reflections, which were then used in the program INDEX to obtain an orientation matrix for data collection and to provide cell dimensions.[28] A periodic remeasurement of three standard reflections revealed a crystal decay, on X-ray exposure, which was evaluated as about 15% for **1a** and 10% for **2a** on F_o at the end of data collection. Lorentz, polarization, decay, and absorption corrections were applied, the last performed with the empirical method described in ref 29. On the basis of unrealistic, although positively definite, refined anisotropic thermal parameters for some of the lighter atoms of compound **1a**, a further absorption correction (DIFABS)[30] was applied to its full data set (vide infra), after complete isotropic refinement.

Solution and Refinement of the Structures for 1a and 2a. The metal atoms were located from three-dimensional Patterson maps, and the coordinates of the remaining non-hydrogen atoms were located by successive least-squares refinements and difference Fourier maps. The refinements were carried out by full-matrix least squares with anisotropic temperature factors for Ir, Hg, Au, P, Cl, and carbonyl groups, while the remaining C and N atoms were refined isotropically, the minimized function being $\sum w(F_o - k\,|F_c|)^2$. Hydrogen atoms were included in the last structure factors calculations, in their ideal positions (C–H = 0.95 Å, B =

---

(28) B. A. Frenz and Associates, SDP Plus Version 1.0, Enraf-Nonius, Delft, The Netherlands, 1980.

(29) North, A. C. T.; Phillips, D. C.; Mathews, F. S. *Acta Crystallogr. Sect. A: Cryst. Phys. Diffr. Theor. Gen. Crystallogr.* **1968**, *A24*, 351.

(30) Walker, N.; Stuart, D. *Acta Crystallogr.* **1983**, *A39*, 158.

7 Å²). Individual weights were given as $w = 1/\sigma^2(F_o)$, where $\sigma(F_o) = \sigma(F_o^2)/2F_o$, $\sigma(F_o^2) = [\sigma^2(I) + (pI)^2]^{1/2}/L_p$, and p, the "ignorance factor", is equal to 0.04 for **1a** and to 0.05 for **2a**. Scattering factors and anomalous dispersion corrections were taken from ref 31. Although some of the thermal amplitudes of terminal carbonyls of compound **1a** even after the DIFABS correction show high anisotropy and a certain amount of along-bond motion (see Figure 2), it was decided to rely on the final fractional coordinates obtained in the anisotropic refinement, as suggested by Braga et al.[32] The small decrease of R_w (0.0469 vs 0.0437) on passing from isotropic to anisotropic carbonyls was however significant on the basis of Hamilton's test[33] at the 0.5% level, for 371 and 521 parameters, respectively. The two refinements showed slight differences in the Ir–C and C–O distances, with a systematic shortening of about 0.02 Å for the Ir–C ones in the isotropic case, due to a possible misplacement of the carbon atoms. A similar effect has been reported.[32b] Three peaks, refined with high (11–17 Å²) isotropic thermal parameters around a crystallographic inversion center in the unit cell of compound **1a** were interpreted as a cyclohexane molecule; an ordered THF molecule was located and refined in the unit cell of compound **2a**. All computations were performed on a PDP 11/73 computer using the SDP package[28] and the physical constants tabulated therein. The positional parameters for compounds **1a** and **2a** are listed in Tables VII and VIII, respectively.

Acknowledgment. We gratefully thank one reviewer for his contribution to the elucidation of the NMR results and layout of the manuscript.

Registry No. 1, 134152-26-4; $1\cdot0.5C_6H_{12}$, 134208-29-0; **2**, 134131-36-5; $2\cdot C_4H_8O$, 134152-24-2; $[N(PPh_3)_2]_2[Ir_6(CO)_{15}]$, 87525-25-5; $[NMe_3(CH_2Ph)]_2[Ir_6(CO)_{15}]$, 76540-42-6; $HgCl_2$, 7487-94-7; $Au(PPh_3)Cl$, 14243-64-2.

Supplementary Material Available: Tables A and E, listing anisotropic thermal parameters for **1a** and **2a**, Tables B and F, giving calculated fractional coordinates of the cation hydrogen atoms for **1a** and **2a**, and Tables D and H, listing distances and angles for **1a** and **2a** (26 pages); Tables C and G, listing structure factors for **1a** and **2a** (72 pages). Ordering information is given on any current masthead page.

---

(31) *International Tables for X-ray Crystallography*; Kynoch Press: Birmingham, U.K., 1974; Vol. 4.

(32) (a) Braga, D.; Koetzle, T. F. *J. Chem. Soc., Chem. Commun.* 1987, 144. (b) Albano, V. G.; Braga, D.; Grepioni, F. *Acta Crystallogr.* 1989, *B45*, 60.

(33) Hamilton, W. C. *Acta Crystallogr.* 1965, *18*, 502.

Cyclometalation of 1-Aza 1,3-Dienes in Reactions with $Ru_3(CO)_{12}$ with Formation of Four- and Five-Membered Azaruthenacycles[1]

Wilhelmus P. Mul, Cornelis J. Elsevier,* Louis H. Polm, and Kees Vrieze

Anorganisch Chemisch Laboratorium, J. H. van 't Hoff Instituut, Universiteit van Amsterdam,
Nieuwe Achtergracht 166, 1018 WV Amsterdam, The Netherlands

Martin C. Zoutberg, Dick Heijdenrijk, and Casper H. Stam

Laboratorium voor Kristallografie, J. H. van 't Hoff Instituut, Universiteit van Amsterdam,
Nieuwe Achtergracht 166, 1018 WV Amsterdam, The Netherlands

Received November 8, 1990

The dinuclear compounds $Ru_2(CO)_6[R^1CH_2CC(H)NR^2]$ (**2a–e**) and $Ru_2(CO)_6[R^1C{=}C(H)CH_2NR^2]$ (**3a,b,d**) are the first isolable products during thermal reactions of $Ru_3(CO)_{12}$ with 1-aza 1,3-dienes $R^1C(H){=}C(H)C(H){=}NR^2$ (R^1,R^2-MAD; R^1, R^2 = CH_3, *i*-Pr (**1a**), CH_3, c-Hex (**1b**), CH_3, *t*-Bu (**1c**), C_6H_5, *i*-Pr (**1d**), C_6H_5, *t*-Bu (**1e**)). Both primary products **2** and **3** contain an isomerized MAD ligand that is part of a four- (**2**) or five-membered (**3**) azaruthenacycle. The molecular structure of **3a** has been solved by X-ray crystallography: space group $P\bar{1}$, with a = 22.511 (4) Å, b = 13.740 (3) Å, c = 12.443 (2) Å, α = 103.21 (1)°, β = 113.00 (1)°, γ = 77.71 (1)°, V = 851.3 Å, Z = 2, and R = 0.027 (R_w = 0.042), for 2540 observed reflections. Compound **3a** contains a formally 6-electron donating enyl–amido ligand and is μ-N,σ-C_β,η^2-C=C-coordinated to a "sawhorse" $Ru_2(CO)_6$ core. In solution both **2** and **3** are stereochemically nonrigid, due to "windshield wiper" motions of the asymmetrically bridged amido ligands. This process is more facile for **2** ($\Delta G^* \approx 35$ kJ mol^{-1}) than for **3** ($\Delta G^* \approx 62$ kJ mol^{-1}), and the ΔG^* value for **3** was shown to be independent of the R^1 and R^2 substituents. In refluxing heptane **2** and **3** are converted into the linear 66-electron cluster $Ru_4(CO)_{10}[R^1C{=}C(H)C(H){=}NR^2]_2$ (**5a–e**), albeit conversion of **2** into **5** proceeded very slowly and incompletely. Conversion of **3** into **5** proceeds via the intermediacy of $(\mu\text{-H})Ru_2(CO)_5[R^1C{=}C(H)C(H){=}NR^2]$ (**4**), which air-sensitive compound could be observed and isolated for R^1, R^2 = C_6H_5, *i*-Pr (**4d**). Reaction of **3a,b** with CH_3,R^2-MAD or crotonaldehyde in heptane at 90 °C results in the formation of $Ru_2(CO)_6[CH_2CC(H)C(H){=}NR^2]$ (**6a,b**). During this conversion the coordinated ligand is dehydrogenated whereas the added substrate acts as a hydrogen acceptor. For crotonaldehyde it was shown that the olefin moiety was hydrogenated chemoselectively. The formation of **2** and **3** out of $Ru_3(CO)_{12}$ and R^1,R^2-MAD and their conversion into **4–6** are discussed.

Introduction

Transition-metal complexes containing a (hetero)-metallacyclopentadiene moiety (A–D) (Figure 1) have attracted attention throughout the years. Interest arises from (i) the versatile coordination behavior of metallacycles in di- and polynuclear compounds,[2] (ii) the electronic

---

* To whom correspondence should be addressed.

(1) Reactions of Monoazadienes with Metal Carbonyl Complexes. 4. Part 3: See ref 7.